10th U. S. National Combustion Meeting
Organized by the Eastern States Section of the Combustion Institute
April 23-26, 2017
College Park, Maryland

The Effect of Heavy Working Fluids on Hydrogen Combustion

Martia Shahsavan[1,], J. Hunter Mack[1]*

[1] *Department of Mechanical Engineering, University of Massachusetts Lowell, 1 University Ave, Lowell, MA, USA*
[*] *Corresponding Author Email: martia_shahsavan@student.uml.edu*

Abstract: The thermodynamic efficiency of internal combustion engines is dependent on the compression ratio and specific heat ratio of the working fluid. Using a mixture of oxygen and noble gases instead of air can increase the thermal efficiency due to their higher specific heat ratio. It also has advantage of eliminating NOx caused by lack of nitrogen. In this study, the three dimensional turbulent injection of hydrogen into a constant volume combustion chamber has been modeled and compared to mixtures of oxygen with nitrogen, argon and xenon. All conditions including the mass flow rate of the injected fuel, injection velocity, and initial temperature and pressure of the chamber were kept constant. The results indicate that the hydrogen jet has more penetration length in nitrogen compared to argon and xenon. However, the smaller penetration lengths lead to more complex jet shapes and larger cone angles. In combination with the higher specific heat ratio, combustion in a noble gas environment results in higher temperatures and OH radical concentrations. Furthermore, mixedness is investigated using mean spatial variation and mean scalar dissipation. Hydrogen in argon shows a better mixing rate compared to nitrogen and xenon due to higher diffusivity.

Keywords: Hydrogen Injection, Non-premixed Combustion Modeling, Argon Cycle, Constant Volume Combustion Chamber

1. Introduction

The ideal thermal efficiency of an internal combustion engine is strongly dependent on the specific heat ratio of the working fluid and the compression ratio (Equation 1). Theoretically, an increase in the ideal thermal efficiency can be achieved by replacing nitrogen with higher specific heat ratio gases such as argon and xenon. These efficiency gains have been roughly demonstrated recently by several groups [1-3]. Moreover, using noble gases in combination with oxygen effectively eradicates NOx from the combustion products due to the lack of nitrogen.

$$\eta = 1 - \left(\frac{1}{r^{(\gamma - 1)}} \right) \tag{1}$$

Using hydrogen as fuel in internal combustion engines has long been of interest to the combustion community [4-6]. Although hydrogen production is still a challenge and there are some obstacles with distribution and storage, a broad flammability range and the elimination of major pollutants make it a potential alternative fuel for use in internal combustion engines. Direct injection can be a beneficial method to utilize hydrogen in engines, as it effectively prevents backfire and increases the possibility of reaching a higher volumetric efficiency since it removes the low H_2 density restriction. There are a

number of studies on hydrogen direct injection with experimental [7-10] and numerical approaches [11-14]. However, the application of hydrogen injection into noble gases as working fluids instead of air, which can enhance the thermal efficiency, is not well understood. In this study, hydrogen injection into a constant volume combustion chamber is modeled. A number of combustion characteristics are investigated for argon and xenon as working fluids and compared to nitrogen to assess their potential as alternatives working fluids to use in internal combustion engines.

2. Methodology

2.1 Numerical setup

A three-dimensional transient simulation of hydrogen injection into a constant volume combustion chamber (CVCC) is implemented. The cylindrical chamber has a 50 mm length and 20mm diameter. The injection duration is 2 ms. The jet behavior and combustion characteristics are considered until 6 ms after the injection event. A constant time step size of 2 μs is selected to clearly observe the jet progress. For turbulence, a Large Eddy Simulation (LES) with Smagorinsky-Lilly sub-grid scale model is applied. A 10-species, 21-reactions CHEMKIN mechanism for hydrogen combustion [15] is coupled with the CFD solver by the Eddy-Dissipation Concept (EDC) model. In three different conditions, nitrogen, argon, and xenon (at 79% by volume) in combination with oxygen (21%) are used to initially fill the chamber. In all cases, injection velocity (100 m/s), initial pressure (20 bar), and initial temperature (1000 K) are kept constant.

2.2 Data analysis

The effect of argon and xenon on combustion characteristics is discussed by recording the history of maximum temperature and maximum OH concentration, which is an appropriate radical representing the presence of a flame. Ignition delay is also investigated and compared with nitrogen by extrapolating the steepest increase of temperature.

To compare the hydrogen jet shape in different working fluids, tip penetration length and cone angle as two important parameters in jet studies are measured using image processing, a powerful tool for evaluating objects, environments, and even motion detection [16-20]. Penetration length is defined as the distance between the jet nozzle and the farthest point along the injection direction involving at least 3% mass fraction of hydrogen. This method is implemented by plotting the pixel intensity along the injection line. The first point with an intensity more than a certain value (200 here) is considered as the jet tip and its distance to the nozzle is called the penetration length. For measuring the cone angle, the jet edge is first detected using multiple image processing filters. Cone angle is then defined by the points on the jet edge which have the longest perpendicular distance with the jet axis.

$$\frac{\sigma}{\xi_m} = \frac{\left\{\left[1/(NP)\right]\sum_{i,j}^{N,P}\left[\xi_{i,j}-\xi_m\right]^2\right\}^{1/2}}{\xi_m} \tag{2}$$

$$\chi_m = \frac{1}{NP}\sum_{i,j}^{N,P}\frac{\left(\nabla\xi_{i,j}.\nabla\xi_{i,j}\right)}{\left(\xi_m/\lambda_D\right)^2} \tag{3}$$

Turbulent combustion is heavily dependent on the mixing rate of fuel and working fluid [21]. To analyze the mixing process, the scalar magnitude should be measured in combination with a characteristic length scale. Equation 2 specifies the mean spatial variation which describes the inhomogeneity of the scalar

population. The mean scalar dissipation quantifies the average magnitude of local scalar gradients and represents the rate of fine-scale mixing (Equation 3). In these equations, ζ is the conserved scalar (e. g. mixture fraction), D is the scalar diffusivity, ζ_m is the average intensity over an N by P pixel region of interest, and λ_D is the strain-limited length scale [22].

3. Results and Discussion

3.1 Temperature and OH concentration

Figure 1 illustrates temperature contours of hydrogen injection into nitrogen, argon, and xenon at different times (2, 4, and 6 ms). As shown, hydrogen combustion in argon generates higher temperatures compared to nitrogen and lower temperatures compared to xenon. This originates from higher specific heat ratio of xenon (1.677) compared to argon (1.667) and nitrogen (1.401).

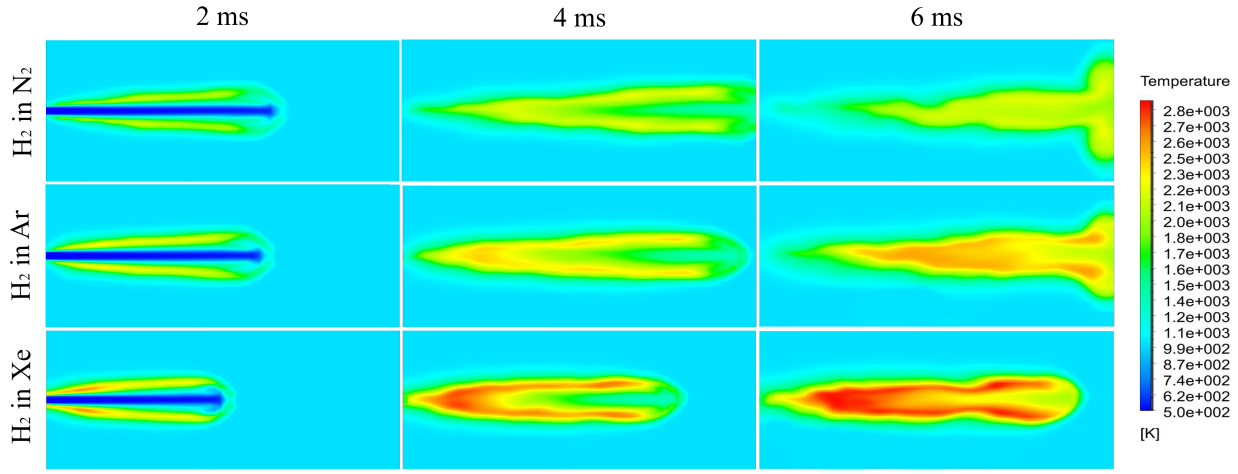

Figure 1. Temperature contours of hydrogen injection into nitrogen, argon, and xenon (From top to bottom) at 2 ms, 4 ms, and 6 ms (From left to right).

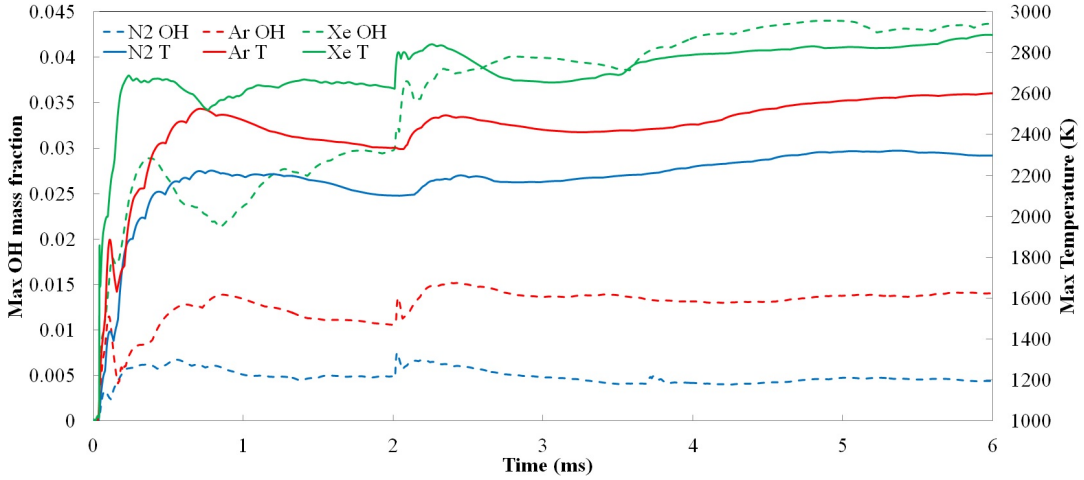

Figure 2. Maximum temperature and maximum OH concentration

The maximum temperature and maximum OH mass fraction versus time for hydrogen injection into nitrogen, argon, and xenon are plotted in Figure 2. The comparison shows that xenon has the highest maximum temperature and OH mass fraction, while nitrogen has the lowest temperature and OH

concentration at all the times. The very early rapid rise in both temperature and OH indicates the ignition and the slight increase at 2 ms is due to the end of injection of the relatively colder fuel stream, better mixing of hydrogen and the working fluid, and generating higher temperatures and OH mass fractions consequently. Figure 2 also indicates that the general trend of temperature and OH histories for each working fluid follow a similar pattern. In order to investigate the ignition delay, the rapid temperature rise region is illustrated in Figure 3. Ignition delay is defined as the time at which temperature grows with the highest rate. Although ignition delay for all cases is around 50 μs, it is slightly shorter for xenon and longer for nitrogen compared to argon. It is also observed that the slope of the temperature curve is higher for xenon and lower for nitrogen when compared to argon.

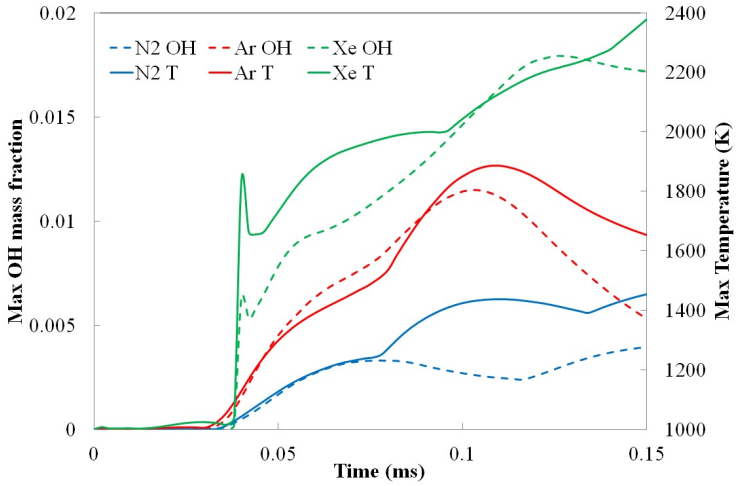

Figure 3. Maximum temperature and maximum OH concentration at early times after injection

3.2 *Penetration length and cone angle*

The time evolution of tip penetration length and cone angle of the hydrogen jet are plotted and compared for the different working fluids in Figures 4 and 5, respectively.

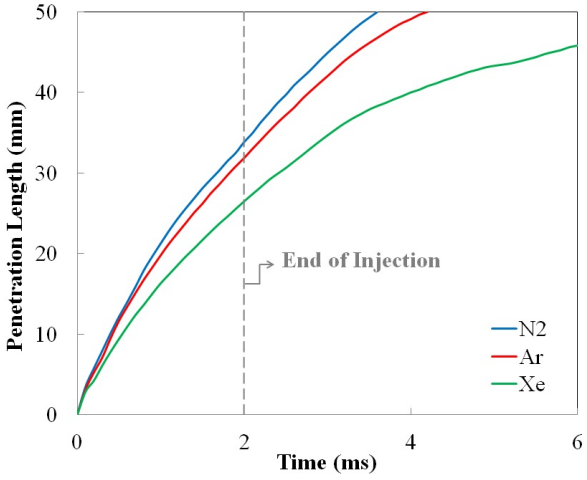

Figure 4. Tip penetration length of hydrogen jet into nitrogen, argon, and xenon

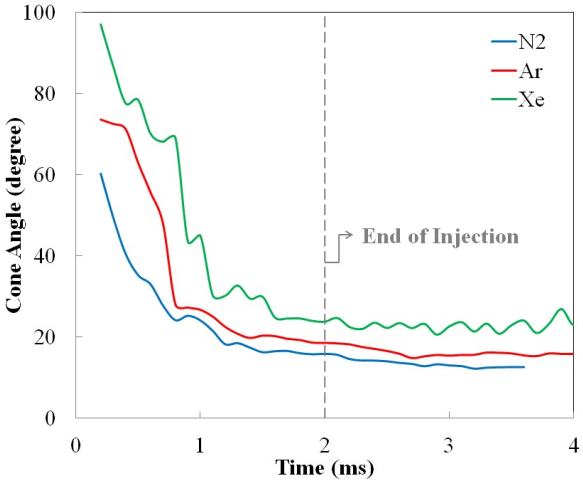

Figure 5. Cone angle of hydrogen jet into nitrogen, argon, and xenon

Nitrogen provides a better environment for penetration of hydrogen due to a lower molecular weight. Thus, the spray cone angle is smaller since the injected mass flow rate is equal for all cases. Contrarily, xenon is the heaviest working fluid and leads to less penetration length of the hydrogen jet and a larger cone angle. Furthermore, it causes more complex jet shapes that can be identified by cone angle fluctuations.

3.3 Mixedness

Equations 2 and 3 are used to evaluate the mean spatial variation and mean scalar dissipation in order to assess the mixedness. These parameters are calculated at every 0.25 ms, giving 24 values for each case. As shown in Figure 6, both mean spatial variation and mean scalar dissipation decrease over time. Although there is no explicit definition of mixedness based on spatial variation versus scalar dissipation plot, it implies that the closer the point to the origin, the better mixing rate of the fuel and the working fluid. To study this concept, equations 2 and 3 are applied to the second half of the injection scenario including 12 values for each case (Figure 7). Argon appears to be the best working fluid compared to nitrogen and xenon since it leads to less spatial variation and scalar dissipation values. This can be justified by higher diffusion coefficient of hydrogen in argon (0.794 cm^2/s at 20℃) compared to its counterparts (0.772 cm^2/s for nitrogen and 0.122 cm^2/s for xenon at the same temperature). Figure 7 also indicates that both the spatial variation and the scalar dissipation drop severely when the jet hits the wall of the chamber due to the flow propagation.

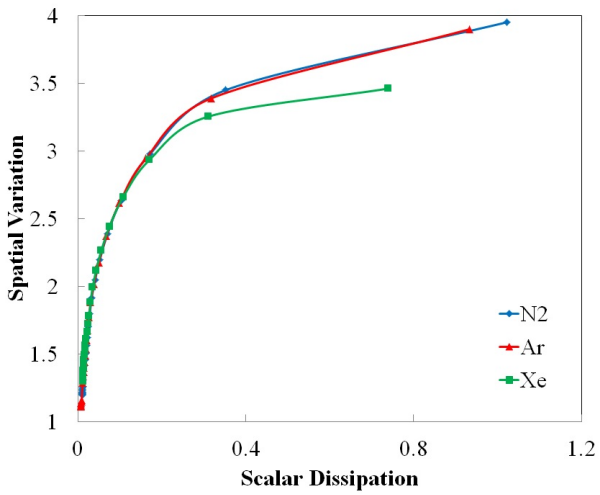

Figure 6. Spatial variation vs. scalar dissipation

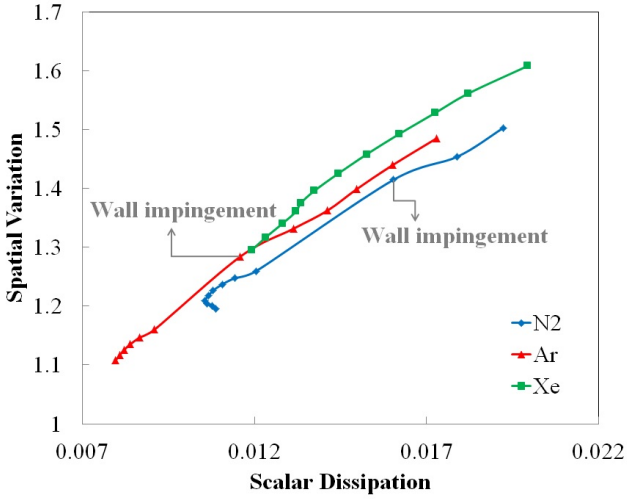

Figure 7. Spatial variation vs. scalar dissipation between 3 ms and 6 ms after injection

4. Conclusions

Typically, higher mixedness and more penetration of fuel into the working fluid provide better conditions for combustion. However, less penetration of fuel inside the chamber and a more complex jet shape combined with a higher specific heat ratio generate higher temperatures during the combustion, resulting in a higher efficiency. Therefore, argon and xenon can be considered as potential alternative working fluids instead of nitrogen. Moreover, utilizing these noble gases eliminates NOx production due to the lack of nitrogen. Argon appears to be a better working fluid for hydrogen combustion, as it provides higher temperatures and OH mass fractions in comparison to nitrogen in addition to a better mixing rate, which is a crucial parameter in non-premixed combustion.

5. Acknowledgements

This research was funded by the University of Massachusetts Lowell. The authors would like to acknowledge the input of Iman Mirzaee Kakhki regarding the numerical model.

6. References

[1] A. Kato, S. Misawa, A. N. M. Yoshimatsu, and D. Sawada, A Study of Rising Thermal Efficiency Using an Argon Circulated Hydrogen Engine, *J. SAE paper,* 20135721, 2013.

[2] N. J. Killingsworth, V. H. Rapp, D. L. Flowers, S. M. Aceves, J.-Y. Chen, and R. Dibble, Increased efficiency in SI engine with air replaced by oxygen in argon mixture, *Proc. Combust. Inst.* 33, no. 2, pp. 3141-3149, 2011.

[3] R. Kuroki, A. Kato, E. Kamiyama, and D. Sawada, Study of high efficiency zero-emission argon circulated hydrogen engine, *SAE Technical Paper*, 0148-7191, 2010.

[4] S. Verhelst, Recent progress in the use of hydrogen as a fuel for internal combustion engines, *Int. J. Hydrogen Energy* 39, no. 2, pp. 1071-1085, 2014.

[5] S. Verhelst and T. Wallner, Hydrogen-fueled internal combustion engines, *Prog. Energy Combust. Sci.* 35, no. 6, pp. 490-527, 2009.

[6] C. White, R. Steeper, and A. Lutz, The hydrogen-fueled internal combustion engine: a technical review, *Int. J. Hydrogen Energy* 31, no. 10, pp. 1292-1305, 2006.

[7] J. G. Antunes, R. Mikalsen, and A. Roskilly, An experimental study of a direct injection compression ignition hydrogen engine, *Int. J. Hydrogen Energy* 34, no.15, pp. 6516-6522, 2009.

[8] A. Mohammadi, M. Shioji, Y. Nakai, W. Ishikura, and E. Tabo, Performance and combustion characteristics of a direct injection SI hydrogen engine, *Int. J. Hydrogen Energy* 32, no. 2, pp. 296-304, 2007.

[9] H. Obermair, R. Scarcelli, and T. Wallner, Efficiency improved combustion system for hydrogen direct injection operation, *SAE Technical Paper*, 0148-7191, 2010.

[10] S. Tanno, Y. Ito, R. Michikawauchi, M. Nakamura, and H. Tomita, High-efficiency and low-NOx hydrogen combustion by high pressure direct injection, *SAE Int. J. Engines* 3, no. 2010-01-2173, pp. 259-268, 2010.

[11] P. Sathiah, E. Komen, and D. Roekaerts, The role of CFD combustion modeling in hydrogen safety management—Part I: Validation based on small scale experiments, *Nucl. Eng. Des.* 248, pp. 93-107, 2012.

[12] N. Smirnov and V. Nikitin, Modeling and simulation of hydrogen combustion in engines, *Int. J. Hydrogen Energy* 39, no. 2, pp. 1122-1136, 2014.

[13] S. Sukumaran and S.-C. Kong, Numerical study on mixture formation characteristics in a direct-injection hydrogen engine, *Int. J. Hydrogen Energy* 35, no. 15, pp. 7991-8007, 2010.

[14] P. Rahnama, A. Paykani, and R. D. Reitz, A numerical study of the effects of using hydrogen, reformer gas and nitrogen on combustion, emissions and load limits of a heavy duty natural gas/diesel RCCI engine, *Applied Energy* 193, pp. 182-198, 2017.

[15] M. Ó Conaire, H. J. Curran, J. M. Simmie, W. J. Pitz, and C. K. Westbrook, A comprehensive modeling study of hydrogen oxidation, *Int. J. Chem. Kinet.* 36, no. 11, pp. 603-622, 2004.

[16] M. Fatouraie, M. S. Wooldridge, B. R. Petersen, and S. T. Wooldridge, Spray Development and Wall Impingement of Ethanol and Gasoline in an Optical Direct Injection Spark Ignition Engine, in *ASME 2015 Internal Combustion Engine Division Fall Technical Conference*, 2015

[17] B. R. Petersen, Transient high-pressure hydrogen jet measurements, Univ of Wisconsin-Madison, 2006.

[18] A. Sarrafi, P. Poozesh, and Z. Mao, A Comparison of Computer-Vision-Based Structural Dynamics Characterizations, Springer, 2017.

[19] P. Zoldak, J. J. Joseph, W. Shelley, J. Johnson, and J. Naber, Characterization of Partially Stratified Direct Injection of Natural Gas for Spark-Ignited Engines, *J. SAE Paper* 0148-7191, 2015.
[20] O. Askari, H. Metghalchi, S. K. Hannani, A. Moghaddas, R. Ebrahimi, and H. Hemmati, Fundamental Study of Spray and Partially Premixed Combustion of Methane/Air Mixture, *J. Energy Resour Tech* 135, no. 2, p. 021001, 2013.
[21] L. Su and N. Clemens, Planar measurements of the full three-dimensional scalar dissipation rate in gas-phase turbulent flows, *Exp. Fluids* 27, no. 6, pp. 507-521, 1999.
[22] D. Probst and J. Ghandhi, An experimental study of spray mixing in a direct injection engine, *Int. J. Engine Res.* 4, no. 1, pp. 27-45, 2003.